(2) *Ibid.*, **68**, 1347 (1979).
(3) H. M. Kalckar, *J. Biol. Chem.*, **167**, 429 (1947).
(4) *Ibid.*, **167**, 445 (1947).
(5) *Ibid.*, **167**, 461 (1947).
(6) J. L. Fox, C. D. Yu, W. I. Higuchi, and N. F. H. Ho, *Int. J. Pharm.*, **2**, 41 (1979).
(7) S. Frederiksen, *Arch. Biochem. Biophys.*, **113**, 383 (1966).
(8) R. A. Lipper, S. M. Machkovech, J. C. Drach, and W. I. Higuchi, *Mol. Pharmacol.*, **14**, 366 (1978).
(9) J. L. York and G. A. LePage, *Can. J. Biochem.*, **44**, 331 (1966).

ACKNOWLEDGMENTS

Abstracted in part from a thesis submitted by C. D. Yu to the University of Michigan in partial fulfillment of the Doctor of Philosophy degree requirements.

Supported by National Institutes of Health Research Grant AI14987 and Training Grant DE00204.

The authors thank Dr. D. C. Baker, University of Alabama, and Dr. A. J. Glazko and Dr. T. H. Haskell, Warner-Lambert/Parke-Davis, for supplying ^{3}H-labeled and nonlabeled vidarabine-5′-valerate ester.

Physical Model Evaluation of Topical Prodrug Delivery—Simultaneous Transport and Bioconversion of Vidarabine-5′-valerate V: Mechanistic Analysis of Influence of Nonhomogeneous Enzyme Distributions in Hairless Mouse Skin

CHENG DER YU *, NEAL A. GORDON, JEFFREY L. FOX, WILLIAM I. HIGUCHI ˣ, and NORMAN F. H. HO

Received August 2, 1979, from the *College of Pharmacy, University of Michigan, Ann Arbor, MI 48109.* Accepted for publication December 13, 1979. *Present address: Syntex Research, Stanford Industrial Park, Palo Alto, CA 94304.

Abstract □ The mathematical problem of simultaneous transport and metabolism in the case of nonuniform enzyme distributions in the skin was solved, and the solutions were used for analyzing experimental data. Experimental data were obtained from permeation experiments with ^{3}H-vidarabine and its 5′-valerate using cellophane tape-stripped hairless mouse skin. Results of the analyses revealed that the esterase activity was four to nine times higher in the epidermis than in the dermis, whereas the deaminase activity was about the same in the two strata. These results were in good agreement with independent experiments using tissue homogenates. The enzyme distributions and the previously reported diffusivities were employed in generating concentration profiles for the prodrug and the drug in the skin. These results may be used in predicting the possible therapeutic effect of the prodrug when it is topically applied.

Keyphrases □ Vidarabine valerate prodrug—topical dosage forms, physical models employing homogeneous and nonhomogeneous enzyme distributions, various mouse skin strata, mathematical analysis □ Prodrugs, topical—simultaneous transport and bioconversion of vidarabine valerate, effect of enzyme distribution and diffusivities on bioavailability, various mouse skin strata, mathematical analysis □ Models, physical—homogeneous and nonhomogeneous enzyme distributions, various mouse skin strata, vidarabine valerate prodrug, topical dosage forms, mathematical analysis

A physicochemical method was developed to determine the *in situ* enzyme rate constants in hairless mouse skin (1, 2). Because of the lack of specific information, preliminary analyses of the experimental data were conducted based on the assumptions of uniform enzyme distribution and constant membrane diffusivities for the substrate and metabolite. It was believed then that when appropriate data became available, a more comprehensive analysis should be conducted based on the possible nonuniform enzyme distributions and the possible variations in diffusivity with respect to position in the membrane.

Subsequent studies were conducted to assess the possible variations in diffusivities and enzyme rate constants. Permeability coefficients of vidarabine (9-β-D-arabinofuranosyladenine, I) in various components of hairless mouse skin were factored out, and the dermis permeability of I was found to be constant throughout the whole stratum (3). Experiments using tissue homogenates revealed (4) that the outer half-thickness of the skin (*i.e.*, the stratum corneum, the epidermis, and part of the dermis) contained more esterase but slightly less deaminase than the remainder of the skin. These data now form the basis for a more comprehensive analysis.

The purposes of the present study were to solve the mathematical problem involved in the simultaneous diffusion and metabolism in the case of the nonuniform enzyme distributions and to analyze the experimental data using these mathematical solutions. The enzyme distributions together with the diffusivities then were employed to generate concentration profiles for the prodrug and the drug in the skin from which the behavior, including the efficacy, of the prodrug may be predicted.

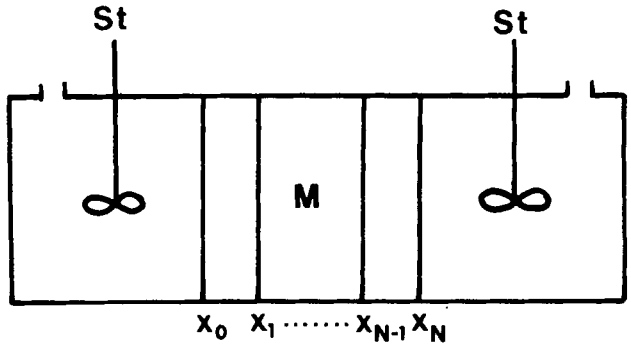

Figure 1—*Multilayer model for simultaneous diffusion and metabolism. Key: M, cutaneous membrane that consists of* N *layers; and St, stirrer.*

0022-3549/80/0700-0775$01.00/0

Table I—Effect of Enzyme Leaching on Observed Fluxes in In-and-Out Experiments with III

Mouse	Pretreatment of Skin Preparation	Flux/Initial Donor Concentration, × 10^6 cm/sec
A	No pretreatment	57.17
B	No pretreatment	66.17
C	Soaking and rinsing for 80 min	29.33
D	Soaking and rinsing for 3 hr	33.67
E	Soaking and rinsing for 3 hr	29.50

Table II—Observed Fluxes in Go-Through Experiments with III Using a Stripped Skin [a]

Running Order[b]	Direction[c]	Flux/Initial Donor Concentration, × 10^6 cm/sec: Donor III	Donor I	Receiver III	Receiver I
Second	Dermis → epidermis	—	17.2	1.20	2.53
First	Epidermis → dermis	—	10.5	1.02	3.01

[a] From a 5-week-old mouse (F). [b] Indicates the first run or the second run with the given skin preparation. [c] Indicates the permeation direction, *i.e.*, from the donor side to the receiver side.

THEORY

General Multilayer Model for Analysis of Simultaneous Diffusion and Metabolism of a Compound—A physical model derived previously (Fig. 2 in Ref. 1) was modified to involve a membrane consisting of N layers (Fig. 1) in which the ith layer has the following properties:

1. Thickness is given by $h_i = x_i - x_{i-1}$.
2. A first-order reaction occurs in this layer, which converts A to B with a rate constant, k_i.
3. Diffusivities of A and B are given by $D_{A,i}$ and $D_{B,i}$.
4. Partition coefficients of A and B are $K_{A,i}$ and $K_{B,i}$.

For generality, aqueous diffusional layers will be considered in a manner similar to the other layers.

Mathematical Solution to Simultaneous Diffusion and Metabolism Problem of Multiple-Layer Model—The differential equations for the steady-state concentrations of A and B in the ith layer are:

$$D_{A,i}\frac{d^2[A]}{dx^2} - k_i[A] = 0 \qquad \text{(Eq. 1)}$$

$$D_{B,i}\frac{d^2[B]}{dx^2} + k_i[A] = 0 \qquad \text{(Eq. 2)}$$

Some new variables may be defined:

$$U_A(x) = \frac{[A]}{K_{A,i}} \qquad \text{(Eq. 3)}$$

$$U_B(x) = \frac{[B]}{K_{B,i}} \qquad \text{(Eq. 4)}$$

$$F_A(x) = -D_{A,i}\frac{d[A]}{dx} \qquad \text{(Eq. 5)}$$

$$F_B(x) = -D_{B,i}\frac{d[B]}{dx} \qquad \text{(Eq. 6)}$$

where $F_A(x)$ and $F_B(x)$ are the fluxes of A and B at x.

Some new constants may be defined:

$$a_i = \sqrt{\frac{k_i}{D_{A,i}}} \qquad \text{(Eq. 7)}$$

$$P_{A,i} = (K_{A,i})(D_{A,i}) \qquad \text{(Eq. 8)}$$

$$P_{B,i} = (K_{B,i})(D_{B,i}) \qquad \text{(Eq. 9)}$$

$$\Delta x = x_i - x_{i-1} \qquad \text{(Eq. 10)}$$

where $P_{A,i}$ and $P_{B,i}$ are the permeability coefficients of A and B, respectively.

The solution of the system in terms of these new variables in the ith layer can be written in matrix form as:

$$\begin{bmatrix} U_A(x) \\ F_A(x) \\ U_B(x) \\ F_B(x) \end{bmatrix} = \begin{bmatrix} \cosh a_i\,\Delta x & \frac{-\sinh a_i\,\Delta x}{P_{A,i}a_i} & 0 & 0 \\ -P_{A,i}a_i \sinh a_i\,\Delta x & \cosh a_i\,\Delta x & 0 & 0 \\ \frac{P_{A,i}}{P_{B,i}}(1-\cosh a_i\,\Delta x) & \frac{\sinh a_i x - a_i\,\Delta x}{P_{B,i}a_i} & 1 & \frac{-\Delta x}{P_{B,i}} \\ P_{A,i}a_i \sinh a_i\,\Delta x & 1-\cosh a_i\,\Delta x & 0 & 1 \end{bmatrix} \cdot \begin{bmatrix} U_A(x_{i-1}) \\ F_A(x_{i-1}) \\ U_B(x_{i-1}) \\ F_B(x_{i-1}) \end{bmatrix} \qquad \text{(Eq. 11)}$$

Table III—Observed Fluxes in Go-Through Experiments with III Using a Stripped Skin [a]

Running Order[b]	Direction[c]	Flux/Initial Donor Concentration, × 10^6 cm/sec: Donor III	Donor I	Receiver III	Receiver I
First	Dermis → epidermis	—	44.6	0.60	0.80
Second	Epidermis → dermis	—	2.59	1.01	1.06

[a] From a 5-week-old mouse (G). [b] Indicates the first run or the second run with the given skin preparation. [c] Indicates the permeation direction, *i.e.*, from the donor side to the receiver side.

Table IV—Observed Fluxes in Go-Through Experiments with III Using a Stripped Skin [a]

Running Order[b]	Direction[c]	Flux/Initial Donor Concentration, × 10^6 cm/sec: Donor III	Donor I	Receiver III	Receiver I
First	Dermis → epidermis	—	41.7	1.64	2.73
Second	Dermis → epidermis	—	18.9	1.82	2.43
Third	Epidermis → dermis	—	2.68	1.50	2.30

[a] From a 5-week-old mouse (H). [b] Indicates the sequence of the runs with the given skin preparation. [c] Indicates the permeation direction, *i.e.*, from the donor side to the receiver side.

Note that if $a_i = 0$, then:

$$-\frac{\sinh a_i\,\Delta x}{P_{A,i}a_i} = -\frac{\Delta x}{P_{A,i}} \qquad \text{(Eq. 12)}$$

and:

$$\frac{\sinh a_i\,\Delta x - a_i\,\Delta x}{P_{A,i}a_i} = 0 \qquad \text{(Eq. 13)}$$

Evaluation of the other terms is straightforward.

Since at $x = x_i$, $\Delta x = h_i$, by denoting the matrix evaluated for $\Delta x = h_i$ by M_i and $U_A(x_i)$ by $U_{A,i}$ and likewise for the other variables, the following is obtained:

$$\begin{bmatrix} U_{A,i} \\ F_{A,i} \\ U_{B,i} \\ F_{B,i} \end{bmatrix} = M_i \cdot \begin{bmatrix} U_{A,i-1} \\ F_{A,i-1} \\ U_{B,i-1} \\ F_{B,i-1} \end{bmatrix} \qquad \text{(Eq. 14)}$$

By applying this relationship repeatedly for $i = 1, \ldots, N$, it follows that:

$$\begin{bmatrix} U_{A,N} \\ F_{A,N} \\ U_{B,N} \\ F_{B,N} \end{bmatrix} = [M_N M_{N-1} \cdots M_2 M_1] \begin{bmatrix} U_{A,0} \\ F_{A,0} \\ U_{B,0} \\ F_{B,0} \end{bmatrix} \qquad \text{(Eq. 15)}$$

where the matrix, $M_N \cdots M_1$, can be shown to have the form:

$$m = \begin{bmatrix} m_{11} & m_{12} & 0 & 0 \\ m_{21} & m_{22} & 0 & 0 \\ m_{31} & m_{32} & m_{33} & m_{34} \\ m_{41} & m_{42} & m_{43} & m_{44} \end{bmatrix} \qquad \text{(Eq. 16)}$$

The solution now is straightforward. From the parameters for each layer, the matrixes, M_i, are evaluated and their product, m, is formed. This matrix then gives the relationship between the steady-state concentrations and fluxes at the two faces of the composite membrane. Determination of fluxes for the go-through and in-and-out experimental conditions is quite simple.

For the go-through experiment where $U_{A,0}$, $U_{A,N}$, $U_{B,0}$, and $U_{B,N}$ are given, it follows from Eqs. 15 and 16 that:

Table V—Least-Squares Fit of Calculated Fluxes to Experimental Data for Determination of Esterase Rate Constants in the Epidermis and the Dermis

		Experimentally Determined[a]	Homogeneous		Nonhomogeneous	
			Two Layer	Three Layer	Two Layer	Three Layer
Iteration parameters[b]						
k_{1e}, $\times 10^3$ sec^{-1}		—	3.35	3.39	9.02	9.27
k_{1d}, $\times 10^3$ sec^{-1}		—	3.35	3.39	1.09	1.06
D_{epi}, $\times 10^9$ cm^2/sec		—	4.55	4.15	4.23	4.40
P_{sc}, $\times 10^3$ cm/sec		—	—	1.28	—	1.80
(Flux/initial donor concentration), $\times 10^6$ cm/sec						
Dermis → epidermis	I (D)[c]	18.9	45.4	45.9	19.2	18.9
	I (R)[c]	2.43	2.43	2.18	2.38	2.36
	III (R)	1.82	1.82	1.70	1.62	1.65
Epidermis → dermis	I (D)	2.68	1.17	1.16	2.77	2.68
	I (R)	2.30	2.43	2.18	2.38	2.36
	III (R)	1.50	1.82	1.70	1.62	1.65
Reflection boundary experiment		19.4[d]	48.5	48.9	22.4	22.1
Σ dev.^{2}		—	2.24	2.23	0.03	0.03

[a] From Table IV. [b] The dermis diffusivity is 1.34×10^{-6} cm^2/sec; the thicknesses of the epidermis and the dermis are 10 and 190 μm, respectively; the aqueous permeability coefficient is 1.08×10^{-3} cm/sec; and the partition coefficient is 1.0. [c] D is the donor chamber and R is the receiver chamber. [d] Average value of the second and third runs from Fig. 2.

$$F_{A,0} = \frac{U_{A,N} - m_{11}U_{A,0}}{m_{12}} \quad \text{(Eq. 17)}$$

$$F_{A,N} = m_{21}U_{A,0} + m_{22}F_{A,0} \quad \text{(Eq. 18)}$$

$$F_{B,0} = \frac{U_{B,N} - m_{31}U_{A,0} - m_{32}F_{A,0} - m_{33}U_{B,0}}{m_{34}} \quad \text{(Eq. 19)}$$

$$F_{B,N} = m_{41}U_{A,0} + m_{42}F_{A,0} + m_{43}U_{B,0} + m_{44}F_{B,0} \quad \text{(Eq. 20)}$$

For the in-and-out experiment where $U_{A,0}$, $U_{B,0}$, $F_{A,N}$, and $F_{B,N}$ are given, it follows from Eqs. 15 and 16 that:

$$F_{A,0} = \frac{F_{A,N} - m_{21}U_{A,0}}{m_{22}} \quad \text{(Eq. 21)}$$

$$U_{A,N} = m_{11}U_{A,0} + m_{21}F_{A,0} \quad \text{(Eq. 22)}$$

$$F_{B,0} = \frac{F_{B,N} - m_{41}U_{A,0} - m_{42}F_{A,0} - m_{43}U_{B,0}}{m_{44}} \quad \text{(Eq. 23)}$$

$$U_{B,N} = m_{31}U_{A,0} + m_{32}F_{A,0} + m_{33}U_{B,0} + m_{34}F_{B,0} \quad \text{(Eq. 24)}$$

In both the go-through and in-and-out experiments, the boundary conditions require that several of the given quantities equal zero so that the equations are somewhat simpler. The matrixes, m, for the two situations are not identical because the go-through experiment has an aqueous diffusional layer on both sides as opposed to only one such layer for the in-and-out experiment.

EXPERIMENTAL

Stripped skin membranes were used for the go-through experiments, and full-thickness skin membranes were used for the in-and-out experiments. Procedures for preparing these skin specimens were described previously (2). The experimental arrangement and procedures for the go-through studies also were described previously (2). The materials were the same as those used previously. 2′-Deoxycoformycin (covidarabine) was used to inhibit the conversion of I to 9-β-D-arabinofuranosylhypoxanthine (II) by adenosine deaminase during the study of esterase activity.

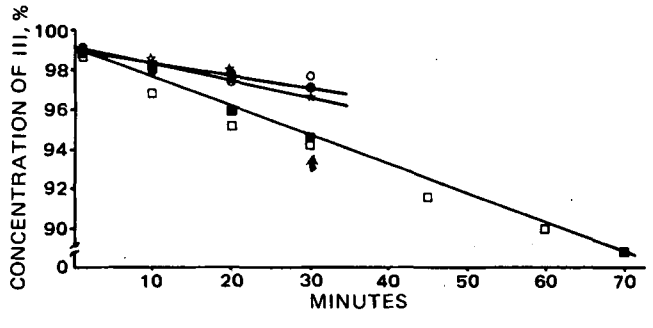

Figure 2—*Consecutive runs of the reflection boundary experiment with III using the same piece of full-thickness skin. The solid symbols are data from Mouse I; the open symbols are data from Mouse J. Lines are the linear regression of data of solid marks. Key:* ■, □, *the first run, which started immediately after preparation, where the arrow indicates the time when the bulk solution was separated from the skin;* ★, ☆, *the second run, which started 2 hr after the zero time of the first run; and* ●, ○, *the third run, which started 1 hr after the zero time of the second run. The system was soaked and rinsed thoroughly with saline between runs.*

RESULTS AND DISCUSSION

Since preliminary data (2) indicated that esterase leaches out from the dermis side of skin, it was desirable to determine if there is a steady level of remaining esterase activity. Therefore, consecutive runs of the reflection boundary experiment with vidarabine-5′-valerate (III) were carried out using a single piece of full-thickness skin (Fig. 2). After 2 hr of leaching, the remaining esterase activity reduced to about one-half of the activity of nonleached skin. An additional hour of leaching did not

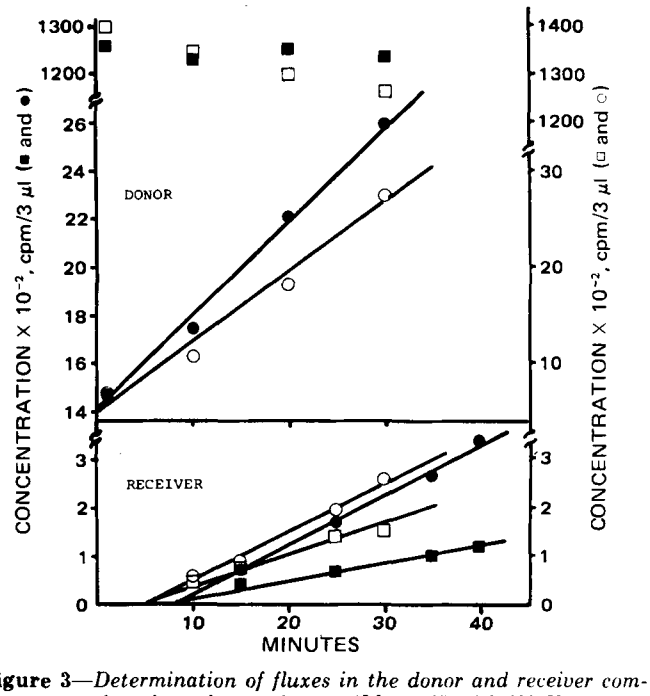

Figure 3—*Determination of fluxes in the donor and receiver compartments of go-through experiments (Mouse F) with III. Key:* ●, ○, *I; and* ■, □, *III. Flux = slope (volume per area), where volume = 1.5 ml and area = 0.713 cm^2. The solid symbols are data of the epidermis → dermis run; the open symbols are data of the dermis → epidermis run. The system was soaked and rinsed thoroughly with saline between runs. Lines are the linear regression of data points.*

Table VI—Least-Squares Fit of Calculated Fluxes to Experimental Data for Determination of Esterase Rate Constants in the Epidermis and the Dermis

		Experimentally Determined[a]	Homogeneous		Nonhomogeneous	
			Two Layer	Three Layer	Two Layer	Three Layer
Iteration parameters[b]						
k_{1e}, $\times 10^3$ sec^{-1}		—	2.07	2.07	3.57	3.56
k_{1d}, $\times 10^3$ sec^{-1}		—	2.07	2.07	1.06	1.11
D_{epi}, $\times 10^9$ cm^2/sec		—	2.36	2.22	2.37	2.36
P_{sc}, $\times 10^3$ cm/sec		—	—	3330	—	23.7
(Flux/initial donor concentration), $\times 10^6$ cm/sec						
Dermis → epidermis	I (D)[c]	21.2	31.6	31.8	18.3	19.0
	I (R)[c]	1.56	1.48	1.38	1.52	1.50
	III (R)	0.87	0.80	0.76	0.76	0.77
Epidermis → dermis	I (D)	1.41	0.68	0.68	1.12	1.11
	I (R)	1.66	1.48	1.38	1.52	1.50
	III (R)	0.49	0.80	0.76	0.76	0.77
Reflection boundary experiment		19.4[d]	33.2	33.2	19.9	20.6
Σ dev.^{2}		—	1.19	1.21	0.30	0.30

[a] Raw data are shown in Fig. 5. [b] The dermis diffusivity is 1.34×10^{-6} cm^2/sec; the thicknesses of the epidermis and the dermis are 10 and 190 μm, respectively; the aqueous permeability coefficient is 1.08×10^{-3} cm/sec; and the partition coefficient is 1.0. [c] D is the donor chamber and R is the receiver chamber. [d] Average value of the second and third runs from Fig. 2.

further reduce the remaining esterase activity. Moreover, as indicated in Fig. 2, the bulk solution after separation from the skin continued to show esterase activity. All of these observations strongly indicate that the leaching of esterase is essentially completed within the first 2 hr. The viability of the skin esterase essentially remains the same for at least 3 hr. Additional data from in-and-out experiments using skin preparations from different mice of the same age gave similar results (Table I).

The leaching effect also was clearly seen in the go-through experiment with nonleached stripped skin. Figure 3 shows the results of two go-through experimental runs carried out consecutively using a single stripped skin preparation (Mouse F). In the first run, the epidermis was in contact with the donor chamber; in the second run, after the system was rinsed thoroughly with saline, the donor and the receiver compartments were reversed so that the dermis side was in contact with the donor chamber. The fluxes[1] for these experiments are given in Table II. Similar experiments with reversed running order (*i.e.*, first run, dermis → epidermis; second run, epidermis → dermis) used stripped skin from another mouse (Mouse G) (Fig. 4 and Table III).

Comparison of Tables II and III reveals that the back-diffusion flux of I was larger when it was obtained from the first run than when it was obtained from the second run, especially for the dermis → epidermis case. The phenomenon was quite reproducible, as was observed in repeat experiments (5). To demonstrate the effect of leaching on the flux determination in a go-through experiment in another manner, a fresh piece of skin (Mouse H) was used for the go-through experiment, as usual, and then, after the system was rinsed thoroughly with saline, the same piece of skin was used for a repeat run (Table IV). Again, there was a twofold difference in the backflow fluxes before and after leaching.

Because of the profound effect of the esterase leaching on the determination of the fluxes, only experimental runs using a preleached skin may give meaningful data for esterase activity determination. Figures 5 and 6 show the results of duplicate runs with preleached skin preparations from the same mouse (Mouse K) conducted by two persons at the

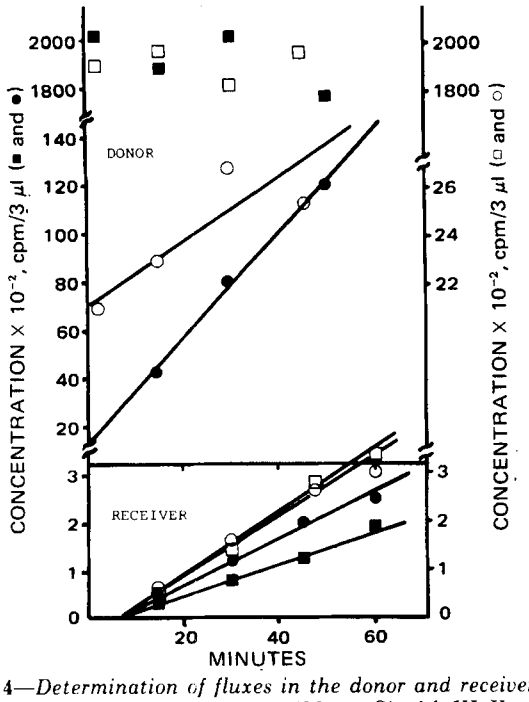

Figure 4—*Determination of fluxes in the donor and receiver compartments of go-through experiments (Mouse G) with III. Key: ●, ○, I; and ■, □, III. Flux = slope (volume per area), where volume = 1.5 ml and area = 0.713 cm^2. The solid symbols are data of the dermis → epidermis run; the open symbols are data of the epidermis → dermis run. The system was soaked and rinsed thoroughly with saline between runs. Lines are the linear regressions of data points.*

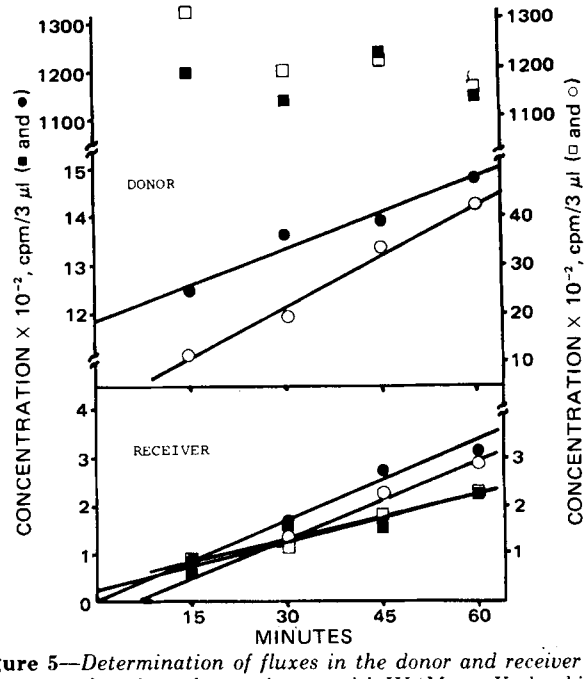

Figure 5—*Determination of fluxes in the donor and receiver compartments of go-through experiments with III (Mouse K; the skin was soaked and rinsed for 3 hr). Key: ■, □, III; and ●, ○, I. Flux = slope (volume per area), where volume = 1.5 ml and area = 0.713 cm^2. The solid symbols are data of the epidermis → dermis run; the open symbols are data of the dermis → epidermis run. The epidermis → dermis run preceded the dermis → epidermis run. The system was soaked and rinsed thoroughly between runs. Lines are the linear regressions of data points.*

[1] All fluxes discussed in this paper are normalized fluxes, *i.e.*, the ratios of fluxes to the initial donor concentration.

Table VII—Least-Squares Fit of Calculated Fluxes to Experimental Data for Determination of Esterase Rate Constants in the Epidermis and the Dermis

		Experimentally Determined[a]	Homogeneous		Nonhomogeneous	
			Two Layer	Three Layer	Two Layer	Three Layer
Iteration parameters[b]						
k_{1e}, $\times 10^3$ sec^{-1}		—	2.14	2.12	4.04	3.92
k_{1d}, $\times 10^3$ sec^{-1}		—	2.14	2.12	0.97	1.02
D_{epi}, $\times 10^9$ cm^2/sec		—	2.24	2.13	2.24	2.23
P_{sc}, $\times 10^3$ cm/sec		—	—	0.59	—	31.8
(Flux/initial donor concentration), $\times 10^6$ cm/sec						
Dermis → epidermis	I (D)[c]	21.2	32.7	32.5	17.0	17.8
	I (R)[c]	1.56[d]	1.37	1.30	1.39	1.39
	III (R)	0.87[d]	0.79	0.76	0.77	0.76
Epidermis → dermis	I (D)	1.90	0.70	0.68	1.24	1.20
	I (R)	1.60	1.37	1.30	1.39	1.39
	III (R)	0.38	0.79	0.76	0.77	0.76
Reflection boundary experiment		19.4[e]	34.2	33.9	18.6	19.3
Σ dev.^{2}		—	2.04	2.06	0.78	0.78

[a] Raw data are shown in Fig. 6. [b] The dermis diffusivity is 1.34×10^{-6} cm^2/sec; the thicknesses of the epidermis and the dermis are 10 and 190 μm, respectively; the aqueous permeability coefficient is 1.08×10^{-3} cm/sec; and the partition coefficient is 1.0. [c] D is the donor chamber and R is the receiver chamber. [d] From Table VI instead of Table VIII because of the unreasonably small permeability in that particular experimental run. [e] Average value of the second and third runs from Fig. 2.

same time. One person conducted experiments in which the epidermis → dermis permeation was run first (Fig. 5), and the other person ran the experiments with dermis → epidermis permeation first (Fig. 6).

The results of the go-through experiments with I using preleached skin (Mouse L) in the deaminase activity determination are shown in Fig. 7. Of the two experiments, the epidermis → dermis permeation preceded the dermis → epidermis permeation.

The following conclusions may be reached from the results using preleached skin:

1. The total fluxes as well as the flux ratio of the two species entering the receiver compartment are independent of direction (*i.e.*, from epidermis side to dermis side or from dermis side to epidermis side).
2. The backflow of metabolite into the donor compartment in the epidermis → dermis run is smaller than that in the reversed direction run.
3. The percentage rates of change in the donor concentrations of III are small. Consequently, these data were not used in the analysis.

Table V lists the results of computer iterations using Eqs. 17–20 to fit the calculated fluxes to the experimental data shown in Table IV. Nonlinear least-squares regression was employed for the best-fit procedure. The analyses were conducted for the nonhomogeneous case in which an epidermis layer was distinguishable from the dermis layer (from the standpoint of diffusivity and esterase activity), in contrast to the homogeneous case in which the two layers were different only in diffusivity and not in esterase activity. In addition to the two-layer model, a three-layer model, taking into account the possible presence of the residual stratum corneum due to incomplete stripping, also was considered.

Three adjustable parameters were involved in the fitting: the epidermis diffusivity, D_{epi}, and the esterase rate constants in the epidermis and the dermis, k_{1e} and k_{1d}, respectively. In the three-layer model, the residual (*i.e.*, if the skin was incompletely stripped) stratum corneum permeability, P_{sc}, is an additional adjustable parameter. The rest of the parameters required for the calculation of fluxes were predetermined experimentally, except for the thickness of the epidermis that was approximated anatomically to be 10 μm.

As seen in Table V, the best-fit iteration parameters under the nonhomogeneous column give calculated fluxes much closer to the experi-

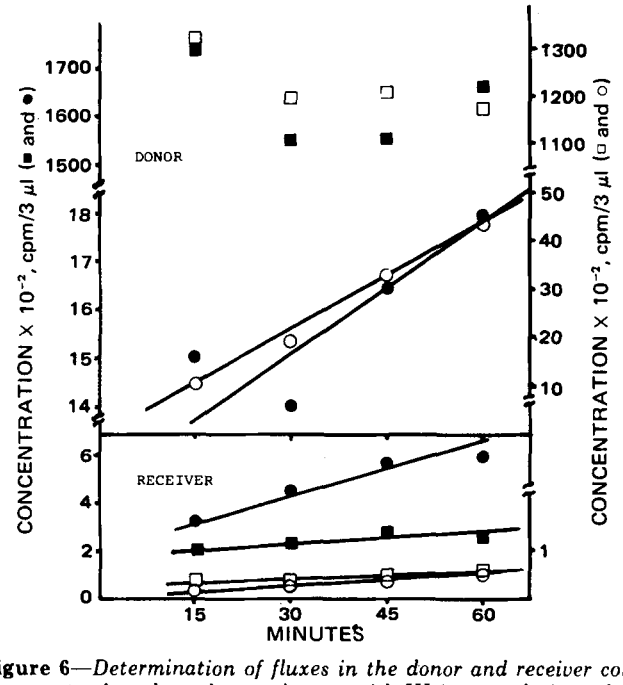

Figure 6—*Determination of fluxes in the donor and receiver compartments of go-through experiments with III (a second piece of abdominal skin from Mouse K; the skin was soaked and rinsed for 3 hr). Key: ■, □, III; and ●, ○, I. Flux = slope (volume per area), where volume = 1.5 ml and area = 0.713 cm². The solid symbols are data of the epidermis → dermis run; the open symbols are data of the dermis → epidermis run. The dermis → epidermis run preceded the epidermis → dermis run. The system was soaked and rinsed thoroughly between runs. Lines are the linear regressions of data points.*

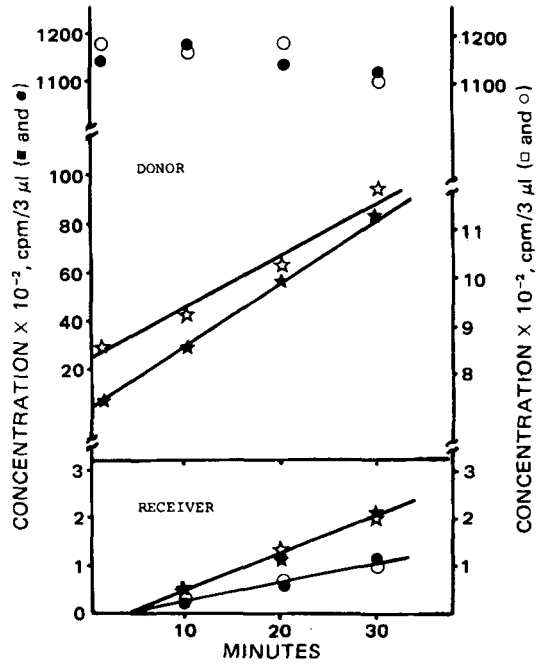

Figure 7—*Determination of fluxes in the donor and receiver compartments of go-through experiments (Mouse L) with I. Key: ★, ☆, II; and ●, ○, I. Flux = slope (volume per area), where volume = 1.5 ml and area = 0.713 cm². The solid symbols are data of the dermis → epidermis run; the open symbols are the data of the epidermis → dermis run. The system was soaked and rinsed thoroughly between runs. Lines are the linear regression of data points.*

Table VIII—Least-Squares Fit of Calculated Fluxes to Experimental Data for Determination of Deaminase Rate Constants in the Epidermis and the Dermis

		Experimentally Determined[a]	Homogeneous		Nonhomogeneous	
			Two Layer	Three Layer	Two Layer	Three Layer
Iteration parameters[b]						
k_{1e}, $\times 10^3$ sec^{-1}		—	7.14	—	7.14	—
k_{1d}, $\times 10^3$ sec^{-1}		—	7.14	—	7.14	—
D_{epi}, $\times 10^9$ cm^2/sec		—	3.00	—	3.00	—
P_{sc}, $\times 10^3$ cm/sec		—	—	—	—	—
(Flux/initial donor concentration), $\times 10^6$ cm/sec						
Dermis → epidermis	II (D)[c]	2.22	2.22	—	2.19	—
	I (R)[c]	1.10	1.13	—	1.12	—
	II (R)	2.30	2.40	—	2.40	—
Epidermis → dermis	II (D)	81.2	77.7	—	78.2	—
	I (R)	1.17	1.13	—	1.12	—
	II (R)	2.42	2.40	—	2.40	—
Reflection boundary experiment		114[d]	90.1	—	90.5	—
Σ dev.^{2}		—	1.16	—	1.17	—

[a] Raw data are shown in Fig. 7. [b] The dermis diffusivity is 1.34×10^{-6} cm^2/sec; the thicknesses of the epidermis and the dermis are 10 and 190 μm, respectively; the aqueous permeability coefficient is 1.08×10^{-3} cm/sec; and the partition coefficient is 1.0. [c] D is the donor chamber and R is the receiver chamber. [d] From Ref. 2.

mental values than do those under the homogeneous column. Thus, the nonhomogeneous model clearly is superior to the homogeneous model. The resultant esterase rate constants, k_{1e} and k_{1d}, reveal an esterase activity that is nine times higher in the epidermis than in the dermis. This result is in good agreement with the previous observation from tissue homogenates (4).

Table V also reveals that the best-fit parameters and calculated fluxes are only slightly different between the two-layer and the three-layer models for both the homogeneous and nonhomogeneous cases. The additional freedom for interaction contributes very little to the goodness of fit as seen from the statistics (Σ dev.^{2}). Moreover, the best-fit values of P_{sc} are on the order of 10^{-3} cm/sec, which is negligible compared to the overall permeability. In other words, the three-layer model essentially regresses to the two-layer model when applied to the present data. The effect of residual stratum corneum is negligible.

Similar analyses for the data shown in Figs. 5 and 6 are given in Tables VI and VII. These analyses lead to the same conclusion.

Results of the deaminase analyses are shown in Table VIII. The analysis based on nonhomogeneous deaminase distribution gave essentially the same results as those based on homogeneous deaminase distribution. The best-fit fluxes gave $k_{2e} = k_{2d} = 7.14 \times 10^{-3}$ sec^{-1}, which is in good agreement with previous observations (4).

The enzyme rate constants thus obtained, together with the transport parameters determined previously (3), give, according to the proposed physical model, the detailed description of concentration profiles of all three species in the viable cutaneous tissue. Figure 8 shows such plots generated from the computer simulation using $k_{1e} = 4.04 \times 10^{-3}$ sec^{-1}, $k_{1d} = 0.97 \times 10^{-3}$ sec^{-1}, $k_{2e} = k_{2d} = 7.14 \times 10^{-3}$ sec^{-1}, and the other required parameters as specified in the legend.

The bioavailability of the topically applied prodrug may be readily assessed quantitatively based on the concentration profiles. The area under the curve of the active parent drug species is ~25% of that of the prodrug species (Fig. 8) in the epidermis where the herpes virus is believed to proliferate. The somewhat low availability of the parent drug in this investigation is primarily due to the relatively slow conversion rate of the prodrug by the esterase. In a theoretical study reported previously (1), the parent drug was ~10 times more abundant than its prodrug when the esterase rate constant was nine times the value of the deaminase rate constant. A high esterase activity becomes a prerequisite in the search for promising prodrug candidates.

Recent studies (6) in this laboratory revealed that the esterase rate constant for the 5-monoesters of I with different chain lengths varies significantly in cultured KB cell suspension systems. The relative rate constants in that study were 22:3:1 for octanoate, valerate, and acetate, respectively. The chain length effect of these esters on the esterase activity of the hairless mouse skin is under investigation.

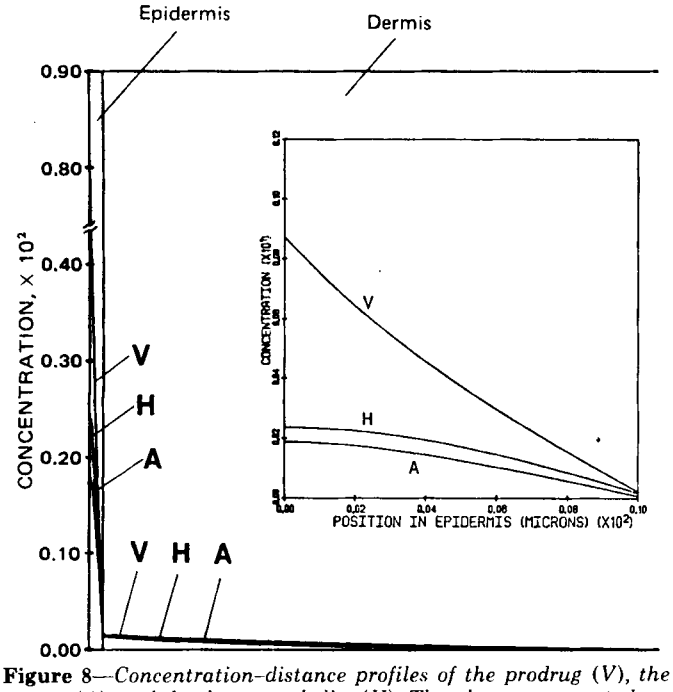

Figure 8—*Concentration-distance profiles of the prodrug (V), the parent (A), and the drug metabolite (H). The plot was generated according to the model using the following parameters: dose on the stratum corneum side of the skin was 1.0 M; diffusivities in the stratum corneum, the epidermis, and the dermis were 1.2×10^{-10}, 2.24×10^{-9}, and 1.34×10^{-6} cm^2/sec, respectively; and thicknesses of the stratum corneum, the epidermis, and the dermis were 40, 10, and 200 μm, respectively. The enzyme rate constants used were described in the text.*

REFERENCES

(1) C. D. Yu, J. L. Fox, N. F. H. Ho, and W. I. Higuchi, *J. Pharm. Sci.*, **68**, 1341 (1979).

(2) *Ibid.*, **68**, 1347 (1979).

(3) C. D. Yu, W. I. Higuchi, N. F. H. Ho, J. L. Fox, and G. L. Flynn, *J. Pharm. Sci.*, **69**, 770 (1980).

(4) C. D. Yu, J. L. Fox, W. I. Higuchi, and N. F. H. Ho, *ibid.*, **69**, 772 (1980).

(5) C. D. Yu, Ph.D. thesis, University of Michigan, Ann Arbor, Mich., 1978.

(6) S. M. Machkovech, W. I. Higuchi, R. A. Lipper, and J. C. Drach, presented at the APhA Academy of Pharmaceutical Sciences, Kansas City meeting, Nov. 1979, Abstract 107.

ACKNOWLEDGMENTS

Abstracted in part from a thesis submitted by C. D. Yu to the University of Michigan in partial fulfillment of the Doctor of Philosophy degree requirements.

Supported by National Institutes of Health Research Grant AI14987 and Training Grant DE00204.

The authors thank Dr. D. C. Baker, University of Alabama, and Dr. A. J. Glazko and Dr. T. H. Haskell, Warner-Lambert/Parke-Davis, for supplying ^{3}H-labeled and nonlabeled vidarabine-5′-valerate ester.